Meanders, eddies and intrusions in the thermohaline front off Northwest Africa

Circulation
Water mass structure
Interleaving
Double diffusion

Circulation
Masse d'eau
Interpénétration
Double diffusion

Eric D. BARTON
Marine Science Laboratories, University College of North Wales, Menai Bridge, Gwynedd LL59 5EY, UK.

Received 23/7/86, in revised form 14/1/87, accepted 31/3/87.

ABSTRACT

The central water mass boundary off Northwest Africa was studied between October 1981 and April 1982. Two cruises surveyed structure of the boundary zone at the start and end of the period, while three moorings monitored currents throughout. The water mass boundary was revealed as a strong thermohaline front of width 10 km with temperature and salinity contrasts of up to 3°C and 1 practical salinity unit, but little density signature. Mean currents observed throughout the period demonstrated the boundary to be associated with a mean alongshore confluence near 22°N, where the Canary current separates from the coast. The front meandered on a scale of 200 km, but also was characterized by meanders and eddies of shorter scales of about 20 km. Early in the observation period, a small anticyclonic eddy drifted across the mooring array, and was followed by passage of the water mass front. Any local convergent circulation relative to the front was too weak to be detectable.

Extensive interleaving was found in the region near the front. In general, intrusion structure was correlated horizontally over distances less than 30 km, but individual layers were found to extend upto 80 km. Cross frontal fluxes due to interleaving were comparable to estimates in other frontal zones, but smaller than eddy flux estimates. A major intrusion was found with properties similar to those expected of intrusions driven by double diffusive fluxes. While these processes were of undoubted importance, it was concluded that the intrusive layer must have originated as a frontal instability. Separation of such large intrusions from the front could represent significant cross frontal transports, and be the source of the isolated water mass nuclei observed in the region.

Oceanol. Acta, 1987, **10**, 3, 267-283.

RÉSUMÉ

Méandres, tourbillons et intrusions dans le front thermohalin au large de l'Afrique nord-occidentale

La limite de l'Eau Centrale a été étudiée au large des côtes de l'Afrique nord-occidentale au cours de deux campagnes qui se sont déroulées au début et à la fin de la période allant d'octobre 1981 à avril 1982, tandis que les courants étaient enregistrés en continu sur trois mouillages. La limite de la masse d'eau est apparue sous la forme d'un front thermohalin très contrasté de 10 km de large avec des écarts atteignant 3°C en température et une unité pratique en salinité, mais avec un contraste peu marqué en densité. L'observation des courants moyens au cours de toute la période a révélé que la limite est associée à une confluence moyenne le long de la côte vers 22°N où le courant des Canaries s'écarte de la côte. Le front formait des méandres à une échelle de 200 km, tout en présentant des méandres et des tourbillons de plus faible extension, de l'ordre de 20 km. Au début de la période d'observation, un petit tourbillon anticyclonique a dérivé à travers la zone des mouillages et a été suivi par le passage du front hydrologique. Aucune circulation convergente locale relative à ce front n'a pu être détectée.

Un important processus d'interpénétration de diverses masses d'eau a été trouvé dans la région à proximité du front. En général, l'intrusion était corrélée horizontalement sur des distances inférieures à 30 km, mais des couches individualisées ont été repérées

jusqu'à 80 km. Les flux traversant le front par processus d'interpénétration étaient comparables aux flux estimés dans d'autres zones frontales, mais inférieures aux estimations du flux turbulent. Une intrusion majeure a été trouvée avec des propriétés semblables à celles propres à des intrusions produites par des flux de double diffusion. Sans nier l'importance de ces processus, nous avons été conduit à la conclusion que la couche d'intrusion devait provenir d'une instabilité du front. La séparation de ces grandes intrusions, du front, pourrait représenter des transports significatifs à travers le front et pourrait être la source des noyaux isolés de masse d'eau observés dans la région.

Oceanol. Acta, 1987, **10**, 3, 267-283.

INTRODUCTION

Open ocean fronts have been frequently noted to be the site of intensive thermohaline structure on vertical scales of less than a meter to more than one hundred meters (*e.g.* Horne, 1978; Joyce *et al.*, 1978). In many cases the front is associated with strong density gradients and along-front baroclinic currents (Gould, 1985; Siedler *et al.*, 1985), but in others the horizontal temperature and salinity differences across the front largely cancel out in their effect on density, as off Northwest Africa (Barton, Hughes, 1982). In that area, a front occurs between the North and South Atlantic central water masses, which occupy the layers from just below the surface down to about 800 m depth. This major water mass boundary extends across the Atlantic, but has been subject to little investigation.

Most observations of the boundary have been made off the African coast near 20°N, incidental to studies of upwelling (*e.g.* Fraga, 1974). The two water masses are characterized by a strong contrast in temperature-salinity (and other) properties, and as one travels equatorward parallel to shore a pronounced decrease in the depth of isotherms and isohalines is experienced over a relatively short distance near Cap Blanc, 21°N (Mittelstaedt, 1982). The changes of temperature and salinity across the boundary in depths close to 200 m can be as large as 3°C and 1 practical salinity unit (psu), while sigma-*t* differences may be hardly noticeable. Interaction between the two water masses is often observed in the form of interleaved layers and isolated structures with intermediate temperature-salinity characteristics (Tomczak, Hughes, 1980).

This paper presents the results of an investigation of the nature of the water mass boundary and its variability during the period October 1981 to April 1982. Particular interest was directed towards determining the relation of the frontal boundary to the regional circulation, observing any indication of organized secondary flow normal to the front, and defining the detailed structure in time and space of intrusive features related to the front. A brief summary of the programme has been presented by Barton (1985).

DATA

The observational programme consisted of two cruises, one in October 1981 and the other in April 1982. An array of moored instruments was left in place during the intervening period. At the start of each cruise, a mesoscale station grid was covered to locate the water mass boundary, and then fine scale sections with station spacings of as little as 1-2 km were made across the boundary. A number of time series stations and drift stations were also carried out in the boundary zone. At each station, a Neil Brown Mark III conductivity/temperature/depth probe (CTD) was used to sample to a depth of 600 m. A General Oceanics rosette sampler mounted 1 m above the probe provided samples for CTD calibration checks. After error checking and calibration, the CTD data were filtered with a running mean over 30 scans, and linearly interpolated to 1 dbar intervals.

Three moorings were placed in a triangle about 30 km apart in approximately 2000 m depth during the first cruise, and recovered during the second. Each mooring carried 6 Aanderaa current meters, each equipped to record conductivity, at 42 m separations above 350 m. Two current meters were affected by fouling, but data return was high, and 14 good conductivity (hence salinity and sigma-*t*) records were obtained. The temperature series were corrected by means of pre- and post-cruise laboratory calibrations, and the conductivity series were corrected by comparison with repeated CTD profiles at mooring launch and recovery. The accuracy of the derived salinity data is about 0.02 psu. Fouling, rotor loss, and failure of the speed channel caused truncation of some velocity records, but ten complete series and seven series between 50 and 95% complete were obtained. Sampling was at 30 min intervals. After error checking and calibration of the records, inertial, tidal and higher frequency fluctuations were eliminated by filtering with a Cosine-Lanczos scheme. The data were then subsampled at 6 hourly intervals.

RESULTS

Background situation

The boundary zone between the two central water masses was found in both October 1981 and April 1982 near Cap Blanc. Its overall orientation, as indicated by the salinity distribution at 150 m depth, was northeast to southwest, but the boundary was characterized by pronounced meandering on a scale of roughly 200 km

Structure of the front

The nature of the boundary was most clearly revealed by a number of sections which cut across it at right angles, *e.g.* the zonal section along 20°30′N in April (Fig. 4). The two water masses were separated by a strong thermohaline front occurring mainly between stations 428 and 429, about 20 km apart. The front was marked by strongly sloping isohalines and isotherms, but much less steeply inclined isopycnals. The maximum horizontal salinity difference of nearly 0.9 psu between adjacent stations, corresponding to a temperature difference of almost 3°C, occurred at a depth of 90 m. The front weakened with increasing depth and sloped down slightly to the west. In this transect, the salinity front extended almost continuously to the surface, but the surface temperature front was weak, and there was no discernible surface density discontinuity.

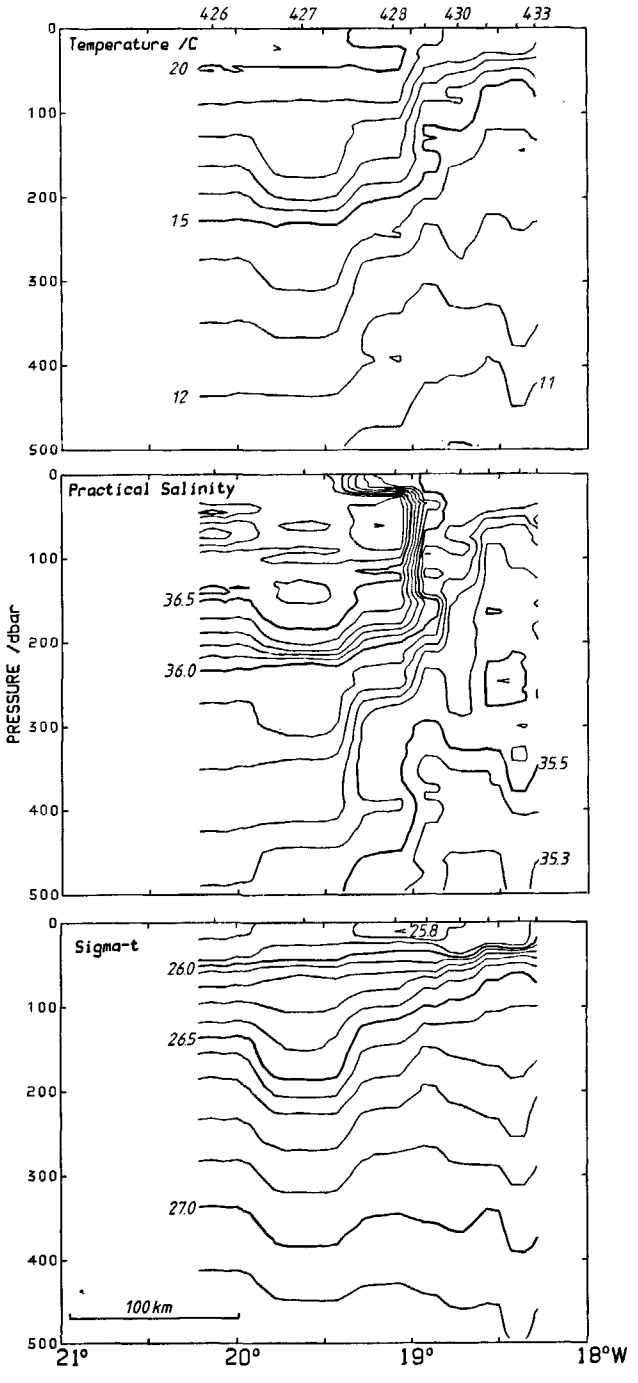

Figure 4
Zonal section of, from top to bottom, temperature, salinity and sigma-t through the water mass front at 20°30′N in April 1982.

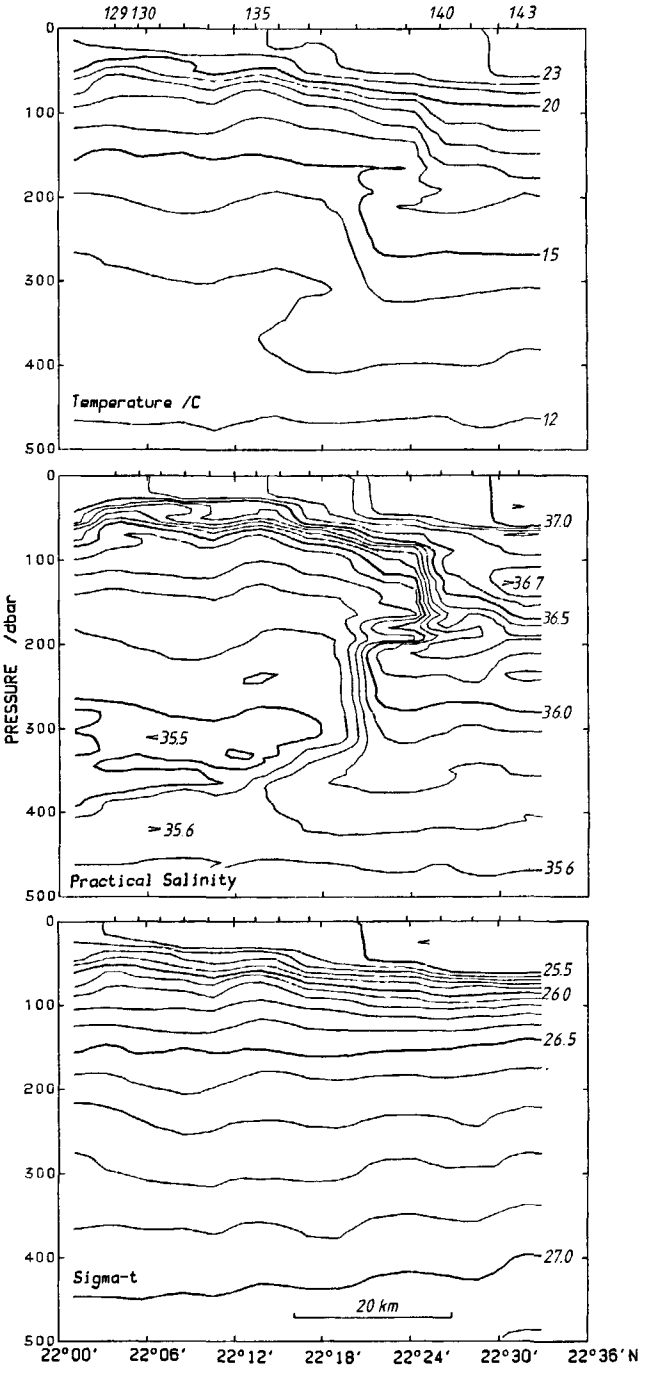

Figure 5
Meridional fine scale section of, from top to bottom, temperature, salinity and sigma-t through the water mass front close to 18 W in November 1981.

One feature of the section was the core of maximum salinity on the NACW side of the front in the upper 100 m. This maximum was found in almost every frontal crossing made during the two cruises. It appears to be related to the meandering of the front. In this section, an anticyclonic meander was indicated by the strong depression of all isopleths at station 427 (*cf.* Fig. 1). Thus, going from east to west across the section, one leaves the SACW, crosses the front (almost at right angles), encounters high salinity NACW, and

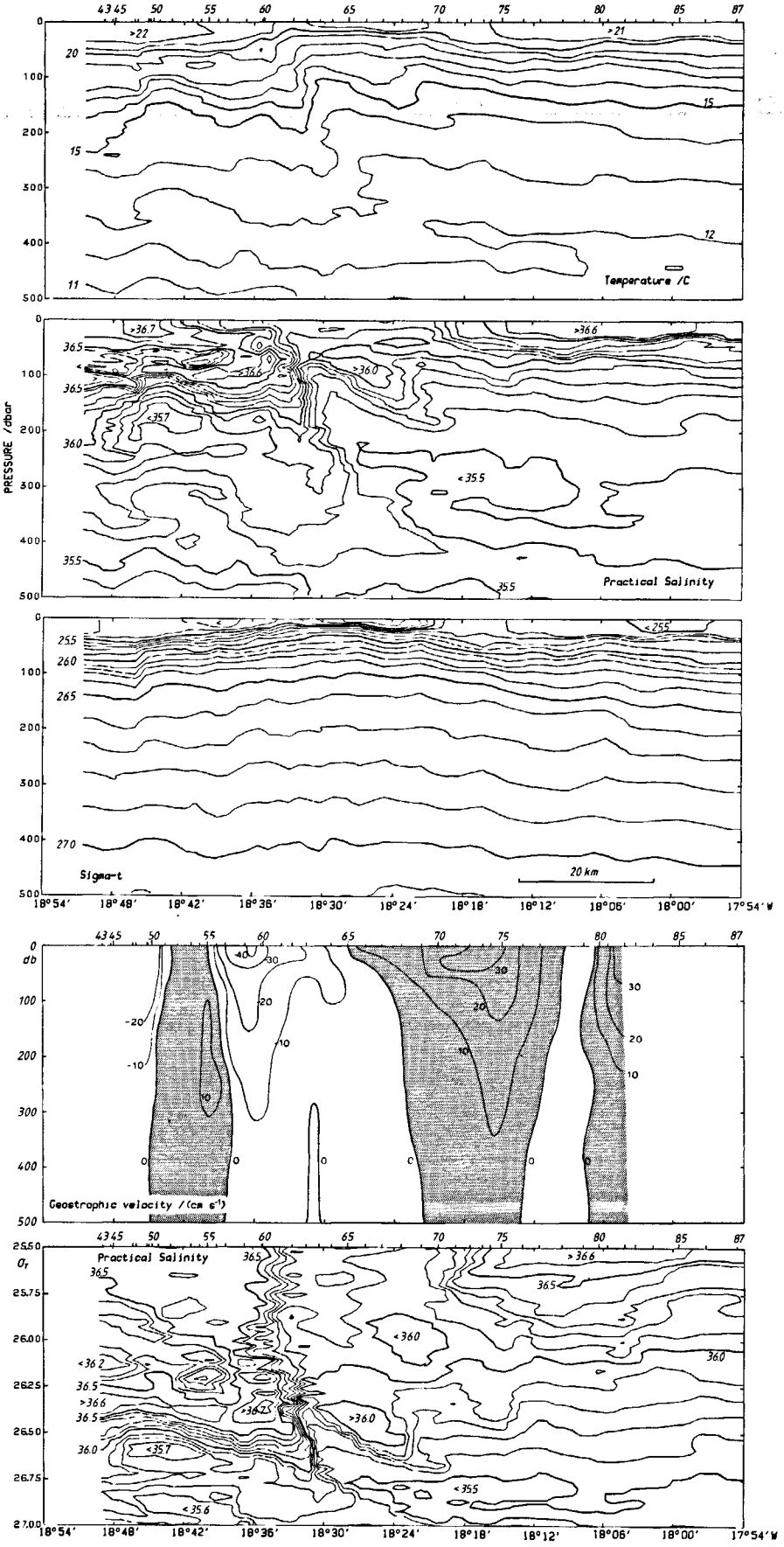

Figure 6

Zonal fine scale section of, from top to bottom, temperature, salinity, sigma-t and geostrophic velocity plotted against depth, and salinity vs sigma-t at 22°N in November 1981. Velocities are in cm s^{-1}, and are shaded to indicate poleward motion.

then begins to detect traces of fresher SACW again, as the western limb of the meander is approached.

Interleaving was indicated by the numerous small inversions and isolated "blobs" of temperature and salinity seen in the section. These appeared concentrated near the front and in the upper 200 m layer. Almost all were seen at one station only, because of the relatively wide spacing of the initial survey stations. Two fine scale sections made in October 1981 at station spacings of a few kilometers resolved the horizontal structure of the front and the interleaving in greater detail.

The first, a 50 km line of 14 stations running from 22°N close to the 18°W meridian, showed the front to be considerably less than 10 km in width (Fig. 5). Over the 4.6 km between stations 139 and 140, temperature and salinity at 150 m depth rose by 2.3°C and 0.7 psu, respectively, while sigma-*t* remained constant. The front did not extend to the surface at this time. In October, warmer surface water masses generally overlay the central waters, as a result of summer heating. The thermohaline or epipycnal nature of the front was particularly clear: there was virtually no density structure coincident with the front. Only a few interleaved features were found, a couple apparently associated with the front itself (stations 138-140 near 200 m depth).

The second fine scale section ran east to west, nominally along 22°N, and terminated close to the southern end of the first. There were 44 stations along the roughly 100 km long transect (Fig. 6). The distributions along this line appeared more complicated than previously seen. The major transition between water masses sloped down towards the east between stations 60 and 65. Its width was again less than 10 km. However, the section did not cut cleanly across the front. At its western end, there was a region of southern, less saline water centred around station 51. Numerous examples of intrusions and inversions were evident across the section, and again no significant density front was apparent in association with the thermohaline boundary. The intrusions and main front are seen in the plot of salinity *versus* sigma-*t*. As in the previous section, the front did not extend to the surface. In the east, there was a reapparance of warm, high salinity water of typically northern characteristics above the SACW.

The density distribution along the section showed a doming of the isopycnal surfaces, which was centred around the main front. The field of geostrophic velocity, computed relative to 500 dbar and smoothed horizontally to suppress variability due to internal waves, revealed essentially a poleward component of flow in the eastern half of the section and an equatorward one in the western half (Fig. 6). This result appeared contrary to the findings of the initial surveys, where flow on both sides of the front was in the same sense.

Meanders and eddies

Refering back to Figure 1, in the initial survey of October 1981, geostrophic flow at 22°N was mainly offshore between 17°30′ and 19°00′W, but meandered north and south as it progressed westward. This same situation applied at the time of the fine scale sections described above. These sections and other stations occupied near the same time provide a more detailed picture of the circulation near 22°N. The dynamic topography of the 150 dbar surface with respect to 500 dbar (Fig. 7) revealed the opposed baroclinic currents of the fine scale zonal section to be limbs of a north-south meander. In the southeast of the area was an anticyclonic eddy of diameter 20 km, while to the north a second, larger anticyclone occurred.

The smaller eddy almost coincided with the position of the three moorings. Currents observed at levels close to 150 m, superimposed on the dynamic topography in Figure 7, also indicated the presence of the eddy. The CTD stations were occupied between 6 and 12 November; the current vectors shown are from 9 November. Change in the current field was slight during the week long survey period. The principal change was that the current vector at C, the northern mooring, rotated anticyclonically from eastward to southward as the eddy shifted westward.

Also shown in Figure 7 is the location of the water mass front, indicated at 150 m by the band of isohalines 35.9 to 36.2 practical units. Although the trends of the front and the flow were similar, the streamlines were not generally parallel to the isohalines. The larger anticyclone appeared to be mainly NACW, but the smaller eddy was situated in SACW. The two eddies were of independent origin rather than having been formed from the same meander. Temperature-

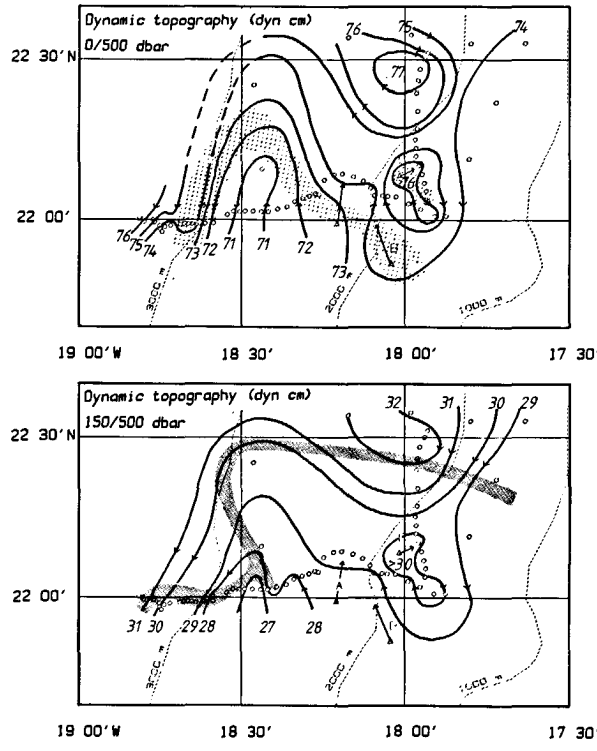

Figure 7

Dynamic topography in dynamic centimetres of (upper) the sea surface, and (lower) the 150 decibar surface relative to 500 decibars. The shaded bands represent the water mass front as indicated by (upper) surface salinities of 36.2-36.5 psu and (lower) salinities at 150 decibars in the range 35.9-36.2 psu. Station positions are shown as circles, and depth contours by dashed lines. Current vectors observed near 150 decibars are shown as arrows at the mooring sites (triangles).

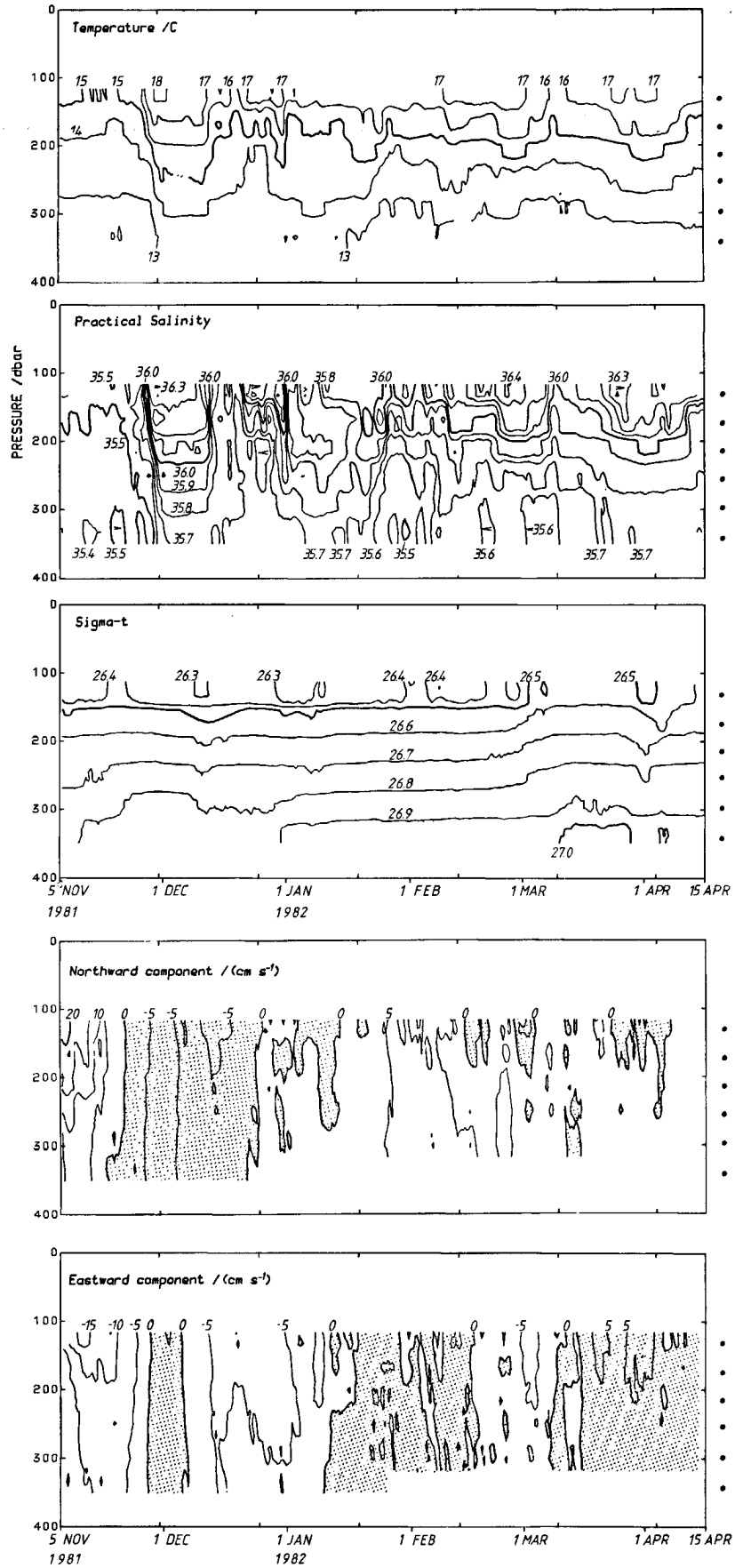

Figure 8

Depth time sections of, from top to bottom, temperature, salinity, sigma-t, northward and eastward velocity observed at mooring B. Observation depths are indicated on the right. Equatorward and eastward flows are shaded.

salinity characteristics from stations near the centre of the smaller eddy, which were among the least saline encountered during either cruise, provided evidence of its southern origin.

The sea surface dynamic topography relative to 500 dbar was similar to that at 150 dbar (Fig. 7). The surface manifestation of the front was significantly displaced from the subsurface boundary, as was evident in the vertical sections. The isohaline band 36.2 to 36.5 marked the region of strongest surface gradient. The front was not well defined by surface temperatures, which showed little contrast in the survey area. At the surface, higher salinity, northern water covered most of the small eddy, but slightly less saline waters were still detectable at its centre. It is possible that the stronger surface currents had wrapped a band of northern water around the eddy, although the station sampling grid was not dense enough to confirm this.

Variability at the moorings

Although in general terms, the situation did not change greatly from October to April, the data from the moorings revealed dramatic fluctuations in the intervening period. The most complete data set, obtained from mooring B, is shown in Figure 8. Observation levels are indicated on the right of each plot.

The large changes which occurred in temperature and salinity were compensating in their effect on density. At the start of the observations, the mooring was located in SACW, but before the end of November the water mass front swept across the array and NACW dominated the rest of the series. The front apparently remained close the mooring B and partially recrossed it on several occasions but the low salinities (<35.5) present at the start never returned. Even at the 40 m resolution offered by the current meters, a number of intrusion-like features were evident in salinity. Indications of interleaving on this scale were also seen in many of the CTD sections. The contours of sigma-*t* were comparatively featureless, except for a gradual increase seen at all depths throughout the observation period. This could be related to a general slight elevation of the density surfaces caused by the spring intensification of coastal upwelling.

Except near the start of the series, currents at mooring B were not much greater than 5 cm s^{-1}, and vertical shears were weak. Fluctuations appeared largely barotropic, *i.e.* changes were in the same sense throughout the depth range. There was no detailed correspondence between variations of temperature or salinity and those in the currents, although periods of equatorward flow tended to coincide roughly with appearances of warm, high salinity water. In particular, there were no obvious velocity changes associated with the passage of the water mass front in November.

Results at the other moorings were qualitatively similar, although there were differences in the timing and intensity of events. The variability at each mooring is summarized in Table 1 as statistics for one current meter close to 170 m depth on each. The kinetic energy of the means is comparable to that found by Gould (1985)

Table 1

Statistics of current observations at levels close to 170 m. Mean and standard deviation of eastward (u, u′ respectively) and northward (v, v′ respectively) velocity components are tabulated along with eddy kinetic energy (EKE) and mean kinetic energy (MKE).

Mooring	Observation depth (m)	u	u'	v	v'	EKE	MKE
		(cm s^{-1})				(cm^2 s^{-2})	
A	176	—4.2	5.3	1.7	6.2	33.3	10.3
B	169	—1.5	4.7	1.5	5.0	23.5	2.3
C	164	—4.2	4.8	—2.0	4.7	22.6	10.8

at 200 m depth in the Azores Front, but the eddy kinetic energy levels are only about one quarter as great. The high correlations of the currents between depth levels are shown in Figure 9, along with correlations between temperature series. Degrees of freedom calculated from estimates of the integral time scale for each series were generally low, but the correlations for both velocity components were always significant. In the case of temperature, correlations decreased rapidly with vertical separation, and were insignificant for the greatest depth differences. This is a reflection of the importance of interleaving, which has a vertical scale smaller than the largest depth interval between current meters.

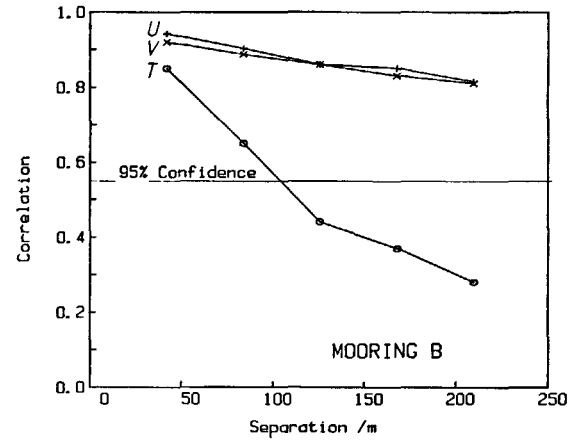

Figure 9

Depth correlations at mooring B of eastward velocity (u), northward velocity (v), and temperature as a function of vertical separation. The 95% confidence level is shown for the correlation with least degrees of freedom.

Movement of the front

It was seen above that during the October-November cruise, the main front at 150 m lay to the north of the moorings, over which was situated a small anticyclonic eddy (*see* Fig. 7). The developments leading to passage of the front across the moorings are shown by a time sequence of current vectors near 170 m depth (Fig. 10). Because of the high vertical coherence, these mid-depth vectors are representative of the currents at all observation levels. Temperature contours estimated by linear interpolation between the moorings are superimposed on the figure. Some caution is necessary in interpretation because curvature of the contours is not defined by the three available observations, yet is significant in the actual fields.

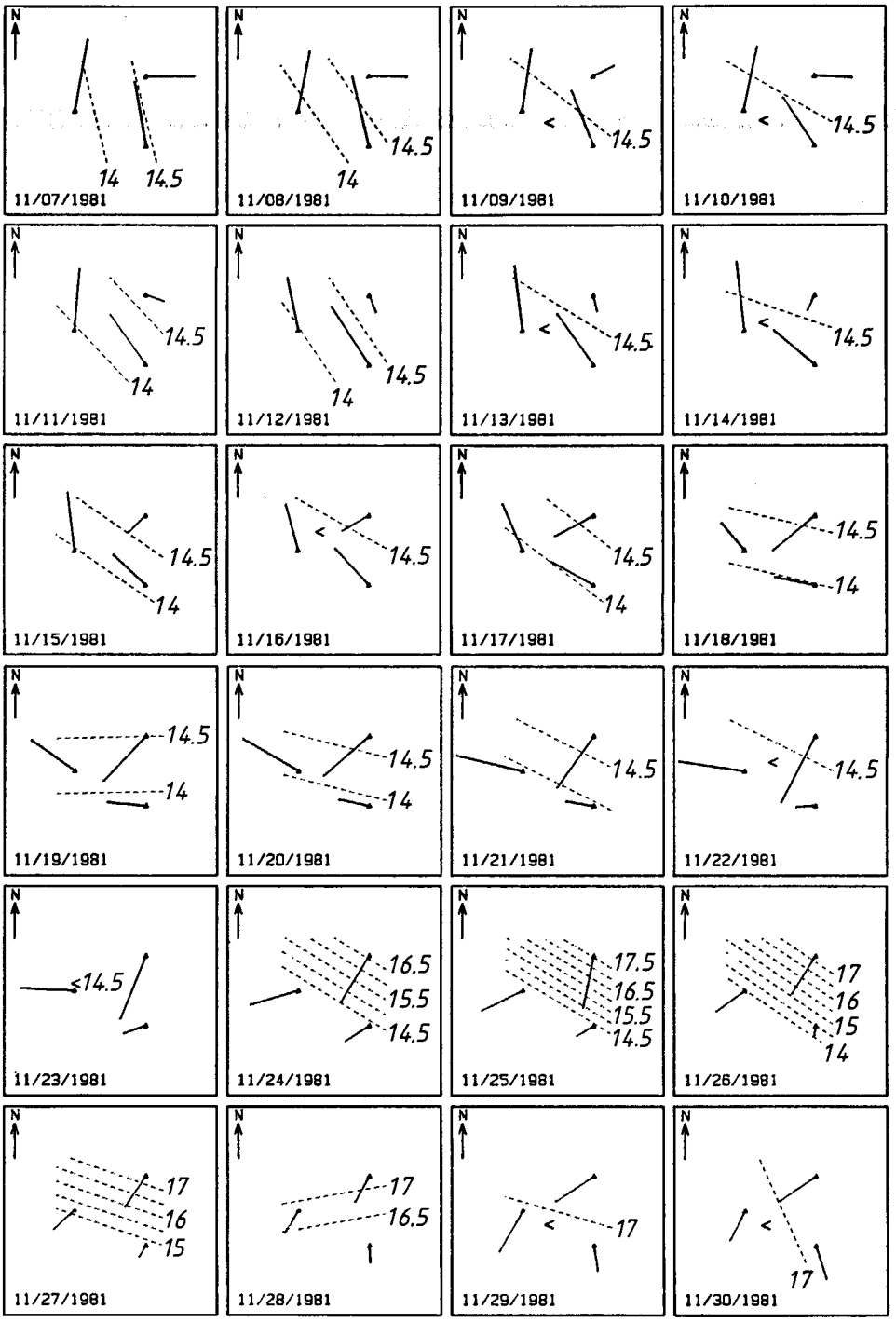

Figure 10

Daily sequence of current vectors observed near 150 m depth at the moorings. The temperature field, linearly interpolated from current meter observations, is superimposed. The length of the North arrow represents 10 cm s^{-1}. Vectors are drawn from the mooring position Δ.

Initially, on 7 November, the eddy appeared to be situated somewhat east of the moorings (Fig. 10), consistent with the sense of rotation of the current vectors and the eastward increase of temperature towards the eddy centre. During the succeeding two weeks, the eddy shifted gradually northwestward. The strongest rotation of the currents occurred at mooring C., which implied that the centre of the eddy passed between sites B and C, and a few days later between A and C. This was supported both by the observed rotation of the temperature field and by the dynamic topography from the fine scale survey (*see* Fig. 7). By 21 November, the eddy had been displaced to the northwest of the array, apparently drifting with the background flow indicated by the dynamic topography. Influence of the eddy, manifested by anticyclonic curvature of the current field, persisted until 26 November, by which time the water mass front had reached the array. The front appeared first at mooring C on 24 November, and traversed the array from northeast to southwest (Fig. 10). The width of the front indicated in the figure is exaggerated by the simple linear interpolation across the array. It took about 5 days for the front to cross the array completely with a speed of

roughly 10 cm s^{-1}, close to that indicated by the current meters. Again, the speed and direction of travel of the front were consistent with advection by the background flow field.

If the front was advected by the background flow, then any strong secondary circulation normal to the front should be revealed by removing the mean velocity as the front crossed any mooring. For the ten day period around passage of the front over each mooring, mean velocities were calculated. Velocity components normal and parallel to the mean flow were found and the mean was subtracted. In every case, a slightly divergent cross-frontal secondary flow was indicated at all levels. This is evident in Figure 10, where the current vectors have a stronger southwestward component before passage of the front than they do after. It may be supposed that, in general, convergent flow is necessary to maintain such a strong front against diffusive effects, even though this did not appear to be the case on this occasion. The considerable uncertainty in defining the "background" or mean flow and the possibly changing "cross-frontal" direction makes it difficult to detect what may be a weak secondary circulation.

From maps similar to those of Figure 10, a number of other eddies were tentatively identified later in the series, but none could be substantiated because of the lack of supporting spatial surveys. The time taken for passage of the later eddies was around ten days. The pattern of variability suggested a succession of meanders and eddy-like features of radius about 20 km progressing past the moorings in a predominantly offshore flow. All of the subsequent events, however, were associated with currents weaker than those in the first eddy.

Intrusive structures

Interleaved "blobs" and intrusions have been noted in many of the frontal sections already, including the time variation seen at mooring B. Reference to Figure 6 reveals impressively complicated salinity and temperature structure, and many inversions 10 to 20 m thick and upto 20 km horizontal extent. Thicker inversions such as the deep salinity minimum persisted over at least 50 km.

The structure in individual temperature and salinity profiles was separated out by high pass filtering in pressure. Structures with vertical wavelengths between 2 and 80 m were retained in the filtered series. The variance of the filtered profiles provides a measure of the amount of structure present in the depth range 0 to 500 m. As expected, most structure was present in profiles close to the front. Least structure was found in profiles in the southern water mass. The temperature and salinity structures were very highly correlated (generally higher than 0.9 in regions of significant structure) as a result of the tendency to be mutually compensating in their effect on density.

Correlations between filtered profiles as a function of spatial separation were calculated. However, because intrusions generally were aligned along sigma-*t* surfaces, correlations were degraded by the substantial depth variation exhibited by these isopycnals as a result of internal wave activity. To overcome this problem, profiles were compared in terms of "stretched pressure" (Joyce *et al.*, 1978). The mean sigma-*t* profile was calculated for the set of stations in question, and the mean pressure value associated with each sigma-*t* value was found. In each of the individual profiles then, the original pressure values were replaced by the mean pressures associated with the observed sigma-*t* values. A plot of, say salinity, against stretched pressure would be similar to a plot against sigma-*t*, except for the advantage that the distortion due to the pycnocline is avoided.

The correlations between adjacent pairs of high pass filtered profiles were calculated for the fine scale zonal line (Fig. 11). Temperature (and salinity) structure was insignificantly correlated over short distances in the immediate vicinity of the front, but elsewhere station to station correlations were high and significant. Intrusive structures generally extended over more than one station, but did not usually extend across the strong front. Ensemble averaged correlations as a function of station separation are shown also in Figure 11. The number of degrees of freedom is high because upto 44 series each with about 30 degrees of freedom enter into calculation of the average correlation at small station separations. The correlation falls to near zero at a separation of about 15 stations because of the influence of the frontal discontinuity. Even so, this is evidence of considerable horizontal persistence of the intrusive structures over distances upto 30 km.

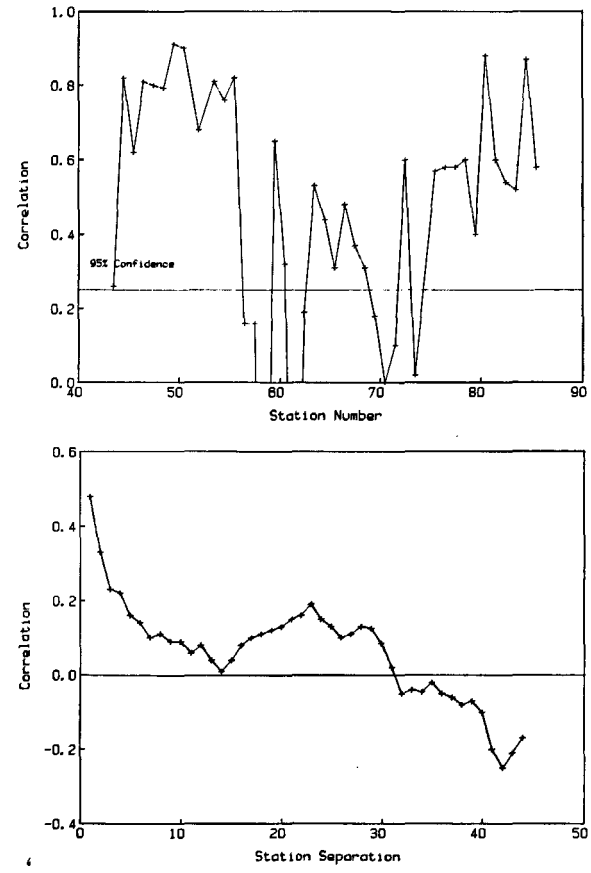

Figure 11

(upper) Correlations between temperature structure at adjacent pairs of CTD stations along the fine section of Figure 6.
(lower) Average correlation of temperature structure along the fine section as a function of station separation.

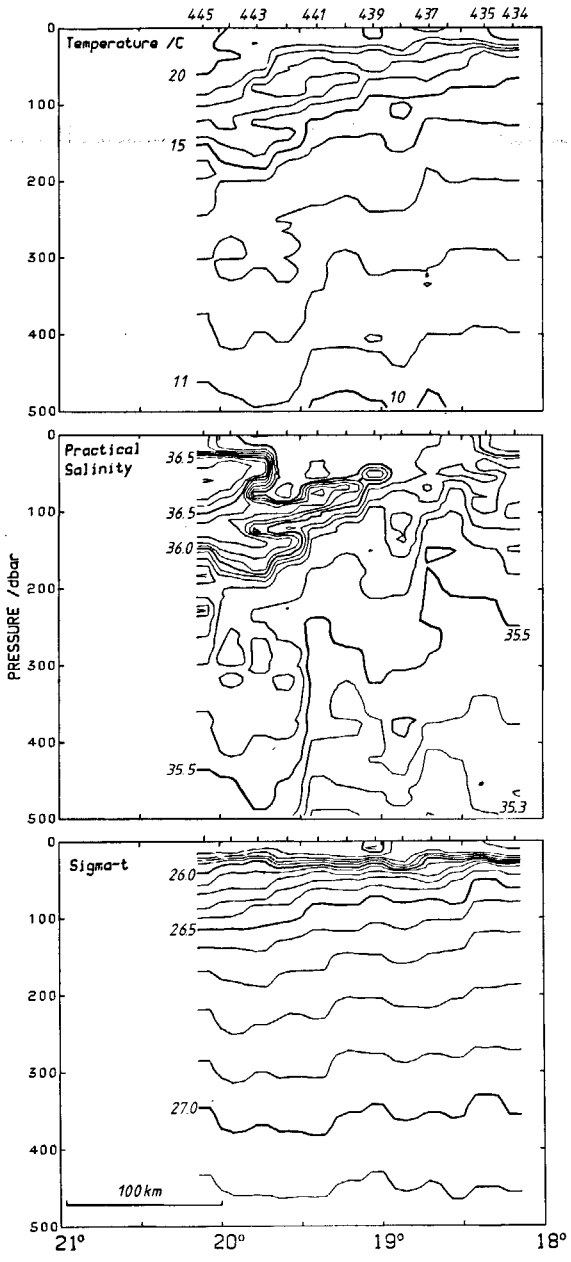

Figure 12
Zonal section of, from top to bottom, temperature, salinity and sigma-t along 20°N in April 1982.

Similar calculations carried out on data from a one day time series station on the NACW side of the front in November 1981 indicated that structures were significantly correlated only for time separations of less than 6 hours. It should be noted, however, that the correlations give a measure of the persistance of structure throughout the observed water column. Degradation of correlation to insignificant values may occur even though particular features at one level are more persistent than indicated by the calculation. Some inversions were in fact traceable over more than 50 km as will be seen below.

A large, warm, salty intrusion

Previous discussion has emphasized the water mass boundary to be a strong front of restricted width, extending almost vertically through the upper 500 m of the water column. In general, little intrusive structure was evident at the front itself. In the April 1982 cruise, however, an unprecedented observation of a huge intrusion of NACW extending from the front was made along 20°N (Fig. 12). The intruding layer was most obvious in salinity, but was also seen in the temperature field. As expected, the temperature and salinity structures were essentially density compensating, so that no density inversion layer occurred. In this section, the form of the front was convoluted with a vertical scale of 60 to 70 m. The intrusion thickness remained constant along most of its roughly 80 km length, although it decreased near the tip. The intrusion shoaled with distance away from the front. Despite a slight upward tilt of the isopycnal surfaces in the same direction, the intruding layer was less dense at greater distances away from the front.

Further observations of the feature were made by sampling with the CTD every half hour while the ship was allowed to drift from an initial position at the root" of the intrusion in the front. During the 18 hour period, the drift was about 13 km south-southwest, almost normal to the front. The observations (Fig. 13) confirmed that the intrusion was a slab-like layer of roughly uniform NACW penetrating into stratified SACW between well defined interfaces in which tempe-

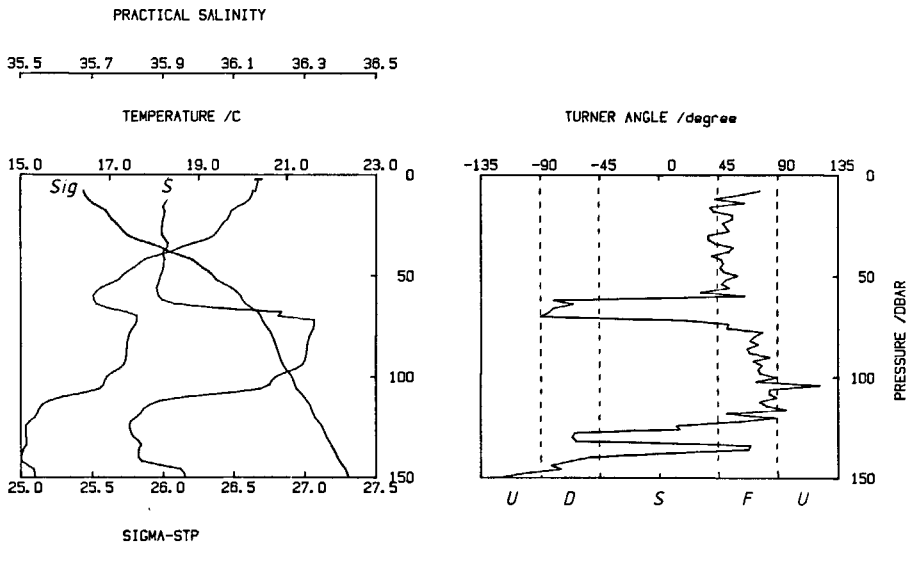

Figure 13
Profiles of (left) temperature, salinity, and sigma-t, and (right) Turner angle, through the large inversion found at 20°N in April 1982.

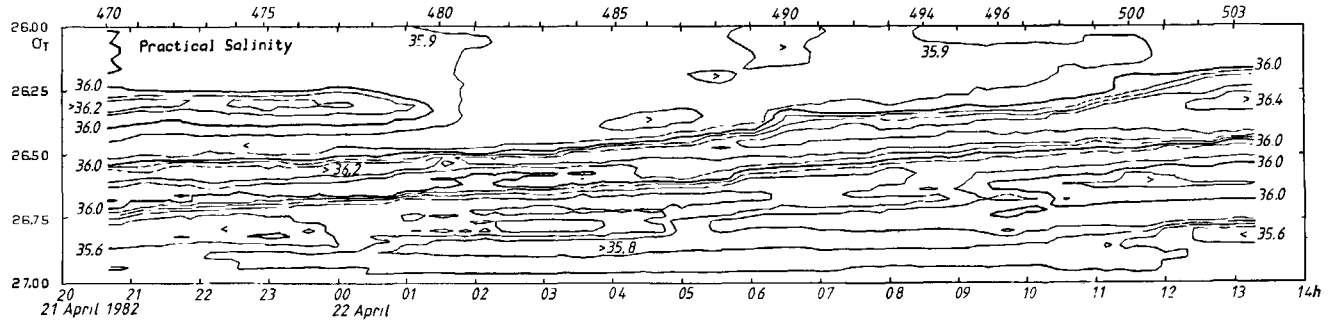

Figure 14
Time variation of salinity vs *sigma-t in the intrusion at 20°N in April 1982.*

rature and salinity changed rapidly in the same sense. Under these conditions, the difference in molecular diffusivities of heat and salt can have significant effect, with the upper interface being suitable for development of double-diffusive convection and the lower for salt fingering. This is supported by the profile of Turner angle (Ruddick, 1983), which reveals regions of intense diffusive activity ($-90 < Tu < -70$) in the upper interface, and intense salt fingering in the lower. Values of the density ratio in the latter case were between 1.1 and 1.4 in general.

A plot of salinity against sigma-*t* reveals the significant rise of the intrusion across density surfaces with increasing distance away from the front (Fig. 14). Also noteworthy is the appearance of a second saline intrusion beneath the principal maximum in the later part of the observations. The shallow salinity maximum seen in the upper left of the figure represents the same feature observed at a similar depth in Figure 12. The three-dimensional extent of the intrusion was not defined by the limited spatial sampling, and there was no opportunity for resampling later to determine temporal changes. However, it had considerable extent both to the east and to the south of the main front, but did not extend as far north as the adjacent section at 20°30′N (*see* Fig. 4).

DISCUSSION

The thermohaline front is obviously a complicated boundary subject to pronounced spatial and temporal variability, incompletely defined by the present observations. Nevertheless, a number of questions may be addressed, albeit in a speculative manner. First, it is of interest to examine horizontal fluxes associated with the front.

The model proposed by Joyce (1977) has been used by a number of workers as a basis for estimating lateral fluxes across interleaving fronts. The horizontal temperature flux is written

$$F_T = \overline{A_T^v \left(\frac{\partial \tilde{T}}{\partial z}\right)^2} \Big/ \frac{\overline{\partial T}}{\partial y},$$

where A_T^v is the vertical diffusivity and the tilde and overbar denote the interleaving and large scale fields, respectively. If A_T^v can be assumed constant, then the flux may be estimated from observed quantities. In particular, the mean square vertical temperature gradient on the interleaving scale is estimated as 2×10^{-3} °C^2 m^{-2} from the vertical profiles high pass filtered as described earlier, while the horizontal gradient is available directly as 3×10^{-4} °C m^{-1}. Taking a value of A_T^v as 10^{-4} m^2 s^{-1} (Joyce *et al.*, 1978) indicates the flux to be 7×10^{-4} °C m s^{-1}. This is similar to the value found by Joyce *et al.* in the Antarctic polar front, and corresponds to a horizontal diffusion coefficient of 2 m^2 s^{-1}. Barton and Hughes (1982) reported a flux greater by a factor of ten on the basis of widely spaced stations during the Auftrieb 75 programme off Northwest Africa. The higher value resulted from sparse sampling indicating weaker horizontal gradients associated with the front. Large uncertainties are associated with the present result because of lack of knowledge of the vertical diffusivity coefficient, which could conceivably range over an order of magnitude. Moreover, Gregg (1980) has pointed out that presence of cross isopycnal motion of intrusions or of vertical double diffusive fluxes, both of which appear most probable, can invalidate the balances assumed in the model.

On longer time scales, the velocity and temperature time series from the moorings also provide temperature flux estimates. Statistics of the velocity component-temperature fluctuations (Tab. 2) indicate significant (at the 95% level) correlations for the meridional component at depths above 200 m on moorings A and B but not at C. Few of the zonal components exhibit significant correlation with temperature. Calculation of the complex correlation coefficient reinforces these results. Significant magnitudes of the coefficient occur only in the upper layers at A and B, while the phase angle indicates near equatorward flux. This is down the regional temperature gradient, since on the whole SACW is cooler than NACW at any level. The size of the corresponding flux ranges between 1×10^{-2} and 7×10^{-2} °C m s^{-1}, the highest values occurring at shallower levels. Fluxes of similar magnitude were reported by Käse *et al.* (1985) for the Azores current front between the Azores and Madeira, and by Gould (1985) south of the Azores. Gould concluded, however, that inadequate sampling in space and time caused discrepancies between moorings in his results. Whether the inconsistency between fluxes at mooring C and the

Table 2

Velocity-temperature correlations at the moorings. The phase angle of the complex correlation is given relative to True North. Correlations significant at the 95% level are starred.

Depth (m)	Number of observations	Correlations $v'T'$	$u'T'$	Complex	Phase angle	Degrees of freedom
Mooring A						
51	326	—0.47	—0.38	0.43	143	20
192	476	—0.63*	—0.42*	0.59*	157	20
134	584	—0.71*	—0.36	0.63*	162	20
176	584	—0.69*	—0.32	0.60*	163	20
219	584	—0.59*	—0.36	0.53*	157	19
261	584	—0.46	—0.31	0.43	157	18
Mooring B						
127	584	—0.44*	0.44*	0.44*	217	23
169	584	—0.49*	0.36	0.45*	208	22
210	584	—0.52*	0.34	0.46*	207	21
251	584	—0.49*	0.19	0.40	197	18
292	522	—0.38	0.19	0.31	202	14
334	301	—0.39	0.05	0.31	185	13
Mooring C						
164	587	—0.24	—0.28	0.27	124	26
206	285	—0.09	—0.39	0.31	99	12
247	584	0.25	—0.48*	0.41	68	20
289	584	0.34	—0.42	0.39	55	20
331	474	0.24	—0.53*	0.43	71	16

others is indicative of inadequate sampling in the present case is problematical. If the results are meaningful, then the eddy flux is one to two orders of magnitude greater than the flux due to interleaving.

A representative value of the velocity-temperature covariance is 2×10^{-2} C m s^{-1}, which is equivalent to 8×10^{4} W m^{-2} as a heat flux. Assuming the eddy heat flux is restricted to the upper 200 m layer where correlations were significant, then the total transport of heat is 1.6×10^{7} W. A typical net heat flux through the sea surface off Northwest Africa is about 150 W m^{-2} (Bowden, 1977). So the eddy heat transport is equivalent to the surface heat transport over an area 100 km by 1 m. If the interleaving heat flux occurs over the upper 500 m layer, the corresponding heat transport is 2×10^{6} W, or an order of magnitude smaller than the eddy heat transport. Transport of heat across the front would then be dominated by the low frequency velocity and temperature fluctuations, which make a contribution to the heat budget of the upper layers comparable to the effects of insolation.

Using the observed mean temperature difference of 0.7°C across the mooring array to define the mean meridional gradient associated with the front, the effective horizontal eddy coefficient may be estimated. With a typical temperature-velocity covariance of 2×10^{-2} °C m s^{-1}, the horizontal eddy diffusivity is greater than 500 m^2 s^{-1}.

It is apparent that the water mass boundary occurs as a result of an alongshore confluence between the equatorward drift of the Canary current and a poleward flow along the Mauretanian coast. If the mean front is governed by a balance between the dissipative tendency of horizontal turbulent diffusion and large scale convergence, then

$$-\gamma y \frac{dT}{dy} = A_H \frac{d^2 T}{dy^2},$$

where γ is the meridional convergence, T is the temperature, and A_H is the horizontal eddy diffusivity. The frontal width L is given approximately by

$$L \simeq 2(A_H/\gamma)^{1/2}$$

(Thorpe, 1983). To a first approximation, the mean front may be considered to lie east-west near the mooring positions. The mean convergence γ is close to 10^{-6} s^{-1}. Using the same data as above indicates a mean frontal width of at least 50 km. Hence an estimate of the eddy coefficient appropriate to the mean front is in excess of 600 m^2 s^{-1}, in agreement with the previous estimate.

In the case of the instantaneous (*i.e.* low pass filtered) front as it crossed the mooring array, there was no evidence of a convergent secondary circulation. Taking the appropriate value of the horizontal eddy coefficient to be 2 m^2 s^{-1}, as indicated by the interleaving flux calculations, and the width of the front to be 10 km, then the expected convergence rate γ is less than 10^{-7} s^{-1}. This corresponds to a difference of only 0.1 cm s^{-1} in the normal velocity component across the front, and would be extremely difficult to detect amongst the many sources of variability. From continuity and assuming uniform conditions in the zonal direction, and no vertical motion at the sea surface, then this would imply a sinking rate of 10^{-5} m s^{-1} or about 1 m/day at a depth of 100 m.

The vertical velocity brought about by cabelling at a density compensated thermohaline front was analyzed by Garrett and Horne (1978), who derived the vertical velocity to be approximately

$$W = -A_H \frac{\partial^2 \rho}{\partial T^2} \left(\frac{\Delta T}{L} \right)^2 \Big/ \frac{\partial \rho}{\partial z}.$$

Taking A_H, ΔT, and L as above and substituting observed values for the density derivatives provides an estimate of the vertical cabelling velocity as 6×10^{-7} m

Table 3
Double diffusive heat and salt fluxes through the interfaces of the large intrusion. Units of heat and salt fluxes are 10^{-5} *°C m* s^{-1} *and* 10^{-5} *psu m* s^{-1}, *respectively.*

	Layer thickness (m)	Temperature step (°C)	Salinity step (psu)	Brunt-Väisälä (10^{-4} s^{-1})	Density ratio	Temperature flux	Salt flux
Diffusive							
Mean	9.4	1.01	0.45	1.20	1.5	5.5	1.2
Stand Devn	4.1	0.17	0.04	0.62	0.3	2.2	0.6
Fingering							
Mean	23.5	—1.87	—0.44	0.37	1.3	6.5	2.7
Stand Devn	7.5	0.20	0.04	0.10	0.1	0.7	0.3

s^{-1} or 0.1 m d^{-1}. These vertical velocities are small and would be masked by background variability. Indeed, the cabelling velocity is so small that it is unlikely to be a mechanism important to maintenance of the convergent front.

In relation to the numerous observations of intrusions and, in particular, the large, warm, salty intrusion, the questions of origin and role arise. It has been pointed out that the well defined interfaces of the intrusions provide conditions in which double-diffusive activity can be important. In the case of the large intrusion, a number of items of circumstantial evidence indicated its behaviour might be influenced by double-diffusive processes. First, the "upper diffusive" interface was more strongly density stratified in terms of the Brunt-Väisälä frequency than the lower "fingering" interface (Tab. 3), as found in laboratory tank studies (Turner, 1978). Second, both interfaces showed intermittent evidence of small scale step structures typical of double-diffusive processes. Third, a deeper saline layer was apparently observed developing beneath the main intrusion, as noted in tank experiments. Fourth, the intruding layer rose across the isopycnal surfaces away from the front, consistent with a net buoyancy gain brought about by dominance of the downward salt fingering flux.

Laboratory experiments have been carried out to determine the heat and salt fluxes through both types of interface (Turner, 1965 and 1967). Subsequent experimental and theoretical studies, *e.g.* Schmitt (1979), indicated some minor adjustments of these results, but McDougall and Taylor (1984) have validated their extension into the parameter range of oceanic interest. A number of authors (*e.g.* Horne, 1978; Middleton, Foster, 1980) have applied the laboratory determinations of flux rates to observations of oceanic step structures and intrusions. In the present case, heat and salt fluxes were calculated for the upper diffusive and lower fingering interfaces utilizing the formulae quoted in the above studies. The results (Tab. 3) correspond to a net density flux out of the layer of about 3×10^{-7} g cm^{-2} s^{-1}. If it is considered that the density decrease along the intrusion was caused by the double-diffusive density flux, then the age of the nose of the intrusion was about 50 days. This is more than an order of magnitude greater than the lifetime of layers estimated by Horne (1978) and by Gregg (1980). Although both the intrusion thickness and the apparent density change are several times larger in this case, such an age is improbable.

The laboratory studies described by Turner (1978) showed that intrusions into stratified media were characterized by the presence of several intruding layers above and below the level of introduction of the anomalous water. Ruddick and Turner (1979) investigated the formation of intrusions from an initial sharp thermohaline density-compensating front in laboratory experiments. They formulated an estimate of the vertical length scale of the intrusions in those conditions:

$$H \simeq 1.5(1-r)\,\beta\,\Delta S \Big/ \left(\frac{1}{\rho}\frac{d\rho}{dz}\right),$$

where ΔS is the salinity contrast across the front. In the present case, the salinity contrast at the depth of the large intrusion is 0.5 to 0.6 practical units. Taking $r = 0.56$ provides a predicted thickness, H, of 77 to 92 m, in fair agreement with the observed vertical scale of 60 to 70 m.

Toole and Georgi (1981), furthering the approach of Stern (1967), explored intrusion formation theoretically for a region of constant thermohaline gradients, *i.e.* a diffuse front. An approximate vertical scale emerged from their study in the form

$$H \simeq 2\pi \left[\frac{N\,\sigma^{1/2} A_S}{0.5(1-r)\,g\,\beta\,\overline{S}_x}\right]^{1/2},$$

where A_S is the eddy diffusivity of salt, σ is the ratio of eddy viscosity to A_S, and S_x is the horizontal salinity gradient. Taking the last to be the salinity contrast across the front divided by the frontal width of approximately 10 km, σ to be in the range 0.1 to 1 following Toole and Georgi, and A_S to be 10^{-3} m^2 s^{-1}, it is found that H lies between 27 and 52 m. This again is in fair agreement with the observed scale (within a factor of two).

The circumstantial evidence makes it appear that the intrusion was affected by double-diffusive processes. Also the scale of the feature was not inconsistent with that predicted by either of the double-diffusive formation theories, although it was impossible to distinguish which one provided better agreement. However, the large horizontal extent of the layer and the indicated age make it highly improbable that the feature was generated solely by the small scale processes. Furthermore, the flux estimates inspire little confidence, even though estimates have been made in similar features before.

A number of factors indicate use of the flux formulae may be inappropriate. The interfaces were one to two orders of magnitude thicker than the experimental tank interfaces. Ample evidence of evanescent smaller scale step structures within the observed interfaces implied that fluxes may have been determined by those more transient features. Structures within the interfaces of stable, well developed layer systems in the Tyrrhenian Sea have been related to salt fingering on the basis of optical evidence (Williams, 1975). Similar phenomena were produced in the laboratory (Linden, 1978), but the behaviour of the overall fluxes was not specified. Other factors are the uncertainty in defining the "mixed" layers separated by the interface, and the possible presence of destabilizing vertical shears in the interfaces. In this latter respect, Barton *et al.* (1982) found that step structures beneath a shallow salinity maximum were of marginal dynamic stability and well developed only when small scale vertical shear was minimal.

A further consideration against the supposition that double-diffusive fluxes dominated the behaviour of the intrusion is that the salinity and temperature in its core increased with distance from the front in the drift series (Fig. 14), instead of decreasing due to fluxes out of the layer. Although it might be argued that the drift track was at an angle to the core of the intrusion, sampling was insufficient to define the horizontal extent and orientation of the layer.

A more plausible alternative is that the intrusion was an advective feature, *i.e.* that it was pulled out from the front by vertical or horizontal shears. The spatial scales are such that internal wave shears would be insufficient. It is likely that some form of baroclinic instability associated with the front is responsible. Woods *et al.* (1977) have suggested one kinematic model relevant to shorter scale (5-10 km) intrusions. The scale of the present intrusion is, however, much larger. In the absence of a sufficiently detailed knowledge of its spatial configuration relative to the front, the specific generation mechanism must remain unclear.

The potential importance of a large intrusion like the present one may be seen. Assuming a temperature anomaly of 0.5°C with respect to the surrounding layers, then the heat content anomaly is 8×10^{16} J. If such an intrusion occurred every 100 km along the front in the upper 200 m layer, then the average anomalous heat content would be 4×10^{11} J m^{-2}. To equal the eddy heat flux of 10^5 W m^{-2}, such intrusions would need to form and break off into the SACW every 4×10^6 s, or about every 40 days. Although the actual separation of intrusions from the front has not been observed, it could explain the observation of large apparently isolated water mass cores in various cruises.

CONCLUDING REMARKS

In summary, the water mass boundary was characterized by strong meandering, eddy activity and intrusions on a variety of scales. The mean front was clarly related to a large scale confluence between the southwestward drifting Canary current and a poleward flow along the continental slope south of Cap Blanc. Detailed hydrographic surveys across the boundary revealed there was a well defined thermohaline front of width about 10 km. No enhanced frontal jet structure in the current field was observed, and no secondary circulation normal to the front was found. Cross frontal fluxes due to interleaving were comparable in magnitude to estimates in other water mass boundary regions, but appeared much smaller than the estimated eddy heat flux, which was comparable to the effect of insolation. In general, inversions and intruding layers were coherent over only relatively short distances and times, but one major intrusion was traceable for about 80 km from the front. Double-diffusive processes were clearly important in transporting heat and salt out of the intrusion, but formation seemed more probably due to instability of the front.

The complexity of the frontal region is such that conventional station sampling is too slow to define the three-dimensional structure of features on the scale of the small anticyclonic eddy and the large intrusion, as well as the context of the larger scale meandering. Improved observations would be possible with a towed depth-cycling CTD system, which would allow more synoptic sampling of the spatial fields and their temporal change. The present lack of information on the structure of the current field could be remedied with the use of Doppler acoustic current profilers, which would permit for the first time an examination of the velocities associated with intrusions. Such observations would allow the significant questions of formation of small eddies and meanders, their development in time, and their role to be investigated in detail.

Acknowledgements

This research was supported by Natural Environment research Council Grant GR3/3522. This programme was initiated under the leadership of Dr. P. Hughes, whose major contribution to the planning and execution of the fieldwork is gratefully acknowledged.

REFERENCES

Barton E. D., 1985. Structure and variability of the central water mass front off Cabo Blanco, *Int. Symp. Upw. W Afr., Inst. Inv. Pesq., Barcelona,* 1, 49-61.

Barton E. D., Hughes P., 1982. Variability of water mass interleaving off NW Africa, *J. Mar. Res.*, **40,** 4, 963-984.

Barton E. D., Hughes P., Simpson J. H., 1982. Vertical shear observed at contrasting sites over the continental slope off NW Africa, *Oceanol. Acta,* **5,** 2, 169-178.

Bowden K. F., 1977. Heat budget considerations in the study of upwelling, in: A voyage of Discovery, edited by M. Angel, *Deep-Sea Res., suppl.,* **24,** 277-290.

Fraga F., 1974. Distribution des masses d'eau dans l'upwelling de Mauritanie, *Tethys,* **6,** 2, 5-10.

Garrett G., Horne E., 1978. Frontal circulation due to cabelling and double diffusion, *J. Phys. Oceanogr.*, **83,** 4651-4656.

Gould W. J., 1985. Physical oceanography of the Azores front, *Progr. Oceanogr.*, **14,** 167-190.

Gregg M. C., 1980. Three dimensional mapping of a small thermohaline intrusion, *J. Phys. Oceanogr.*, **10,** 1468-1492.

Horne E., 1978. Interleaving at the subsurface front in the slope water off Nova Scotia, *J. Geophys. Res.*, **83,** 3659-3667.

Joyce T., 1977. A note on the lateral mixing of water masses, *J. Phys. Oceanogr.*, **7,** 626-629.

Joyce T., Zenk W., Toole J., 1978. The anatomy of the Antarctic polar front in the Drake passage, *J. Geophys. Res.*, **83,** 6093-6113.

Käse R. H., Zenk W., Sanford T. B., Hiller W., 1985. Currents, fronts and eddy fluxes in the Canary Basin, *Progr. Oceanogr.*, **14,** 231-257.

Linden P. F., 1978. The formation of banded salt finger structure, *J. Geophys. Res.*, **83,** 2902-2912.

Manriquez M., Fraga F., 1982. The distribution of water masses in the upwelling region off Northwest Africa in November, *Rapp. PV Réun. Cons. Inter. Explor. Mer,* **180,** 39-47.

McDougall T. J., Taylor J. R., 1984. Flux measurements across a finger interface at low values of the stability ratio, *J. Mar. Res.*, **42,** 1-14.

Middleton J. H., Foster T. D., 1980. Fine structure measurements in a temperature compensated thermocline, *J. Geophys. Res.*, **85,** 1107-1122.

Mittelstaedt E., 1982. The upwelling area off Northwest Africa. A description of phenomena related to coastal upwelling, *Progr. Oceanogr.*, **12,** 307-331.

Ruddick B. R., 1983. A practical indicator of the stability of the water column to double-diffusive activity, *Deep-Sea Res.*, **30,** 1105-1107.

Ruddick B. R., Turner J. S., 1979. The vertical length scale of double diffusive intrusions, *Deep-Sea Res.*, **26,** 903-913.

Schmitt R. W., 1979. Flux measurements on salt fingers at an interface, *J. Mar. Res.*, **37,** 419-436.

Siedler G., Zenk W., Emery W. J., 1985. Strong current events related to a subtropical front in the Northeast Atlantic, *J. Phys. Oceanogr.*, **15,** 885-897.

Stern M., 1967. Lateral mixing of water masses, *Deep-Sea Res.*, **14,** 747-753.

Stramma L., 1974. Geostrophic transport in the warm water sphere of the eastern subtropical North Atlantic, *J. Mar. Res.*, **42,** 537-558.

Thorpe S. A., 1983. Benthic observations on the Madeira Abyssal plain: fronts, *J. Phys. Oceanogr.*, **13,** 1430-1440.

Tomczak M., Hughes P., 1980. Three dimensional variability of water masses and currents in the Canary current upwelling region, "*Meteor*" *Forschungsergebnisse, Reihe A,* **21,** 1-24.

Toole J. M., Georgi D. T., 1981. On the dynamics and effects of double-diffusively driven intrusions, *Progr. Oceanogr.*, **10,** 123-145.

Turner J. S., 1965. The coupled transports of salt and heat across a sharp density interface, *Inter. J. Heat. Mass Transf.*, **8,** 759-769.

Turner J. S., 1967. Salt fingers across a density interface, *Deep-Sea Res.*, **14,** 599-611.

Turner J. S., 1978. Double-diffusive intrusions into a density gradient, *J. Geophys. Res.*, **83,** 2887-2896.

Williams A. J., 1975. Images of ocean microstructure, *Deep-Sea Res.*, **22,** 811-829.

Woods J. D., Wiley R. L., Briscoe M. G., 1977. Vertical circulation at fronts in the upper ocean, in: A voyage of Discovery, edited by M. Angel, *Deep-Sea Res., suppl.,* **24,** 253-275.